

# Investigating the Effect of Process Parameters and Optimizing the Build Time and Material Usage in FDM Using CURA.

Gowtham K S<sup>1</sup> Soundararajan R<sup>2</sup> Sugan V<sup>3</sup> Elayaraja R<sup>4</sup>

<sup>1</sup>PS Scholar <sup>2,3,4</sup>Assistant Professor

<sup>1,2,3,4</sup>Department of Mechanical Engineering

<sup>1,2,3,4</sup>Mahendra Engineering College, Mallasamudram, Namakkal, Tamilnadu, India

**Abstract**— Fused Deposition Modelling (FDM) is one of the most popular Additive Manufacturing (AM) techniques for 3D printing. However, FDM is a complex process and based on many process parameters. Any small change in its process parameters can influence the part printing quality and material properties. There are limited investigations have been reported for exploring the effects of FDM process parameters on 3D printed parts. Therefore, it is crucial to investigate FDM process parameters to ensure the better quality of the 3D printed parts and to ensure this technology is successful for engineering applications. One of the most significant parameters of the FDM for 3D printing process is the raster angle and it is vital to investigate its effect on mechanical properties of 3D printed part. In this study, the five different raster angles are used to fabricate the 3D parts, and their tensile properties are investigated to identify the best raster position to fabricate the strongest 3D printing part. In this study, thermoplastic material - polylactic acid (PLA) is used. In this study, the micro structural analysis on fracture interface of the parts after tensile testing is performed using a scanning electron microscopy (SEM) to explain material failure modes and reasons. In this study, the micro-level structural changes on outer and inner surfaces of the 3D parts that are fabricated using the five different raster orientations are also examined in detail. This study identified the best raster orientation to lie down the layers of 3D printing material during the process. This study also identified that there are several defects in 3D printed parts at micro level that have large impact on mechanical properties of 3D printed part.

**Keywords:** 3D Printer, PLA, Fused Deposition Modelling (FDM), Additive Manufacturing (AM), Microstructural Analysis, Raster Angles, Scanning Electron Microscopy (SEM), Tensile Test

## I. INTRODUCTION

Additive Manufacturing (AM) is a process that can join materials in an additive way (layer upon layer) to make complex physical parts from 3D digital models. This manufacturing technique can be categorised into three fundamental groups such as liquid based, solid based and powder based. Liquid based AM technique construct an object in liquid or high viscose material state and then use heat to harden the object such as material jetting and VAT Photopolymerization [1]. Solid state AM technique use solids in one form or another to create an object such as fused deposit system and Ultrasonic consolidations [2], [3]. Powder based AM technique such as powder bed fusion (PBF) methods use either a laser or electron beam to melt and fuse material powder together [4], [5].

3D printing, is referred to as solid state AM technique, is a process of making an object in three

dimensions by stacking up multiple best thin layers of selected material. The first step of this process is to produce a digital model using a CAD software and transfer it into the 3D printer machine to turn it into a physical object [6]. This technology becomes more famous for fast manufacturing process for the small industries and personnel usage. The most significant advantage for 3D printing is that it can speed up the production process compared to the traditional method of manufacturing [7]. Complicated designs can be uploaded from a SolidWorks software in digital forms to the 3D printers and can be printed in a few hours' time [8]. This technology can be applicable in various fields such as medical sciences [9],[10], construction, automotive, aerospace and architecture [11]–[13]. It has great potential in the medical industry. A Kumar et al elucidated the scope of 3D printing technology for tissue engineering such as development of 3D scaffolds for tissue regeneration [14]–[16]. These studies also discussed the biocompatibility and mechanical properties of 3D scaffolds that are fabricated with different 3D additive manufacturing approaches and concluded that the technology is envisaged to meet the requirements of the biomedical industry. However, some of these applications are still under investigation and considerable research is required to improve their product performance. Moreover, one of the biggest advantages of the materials used for the additive manufacturing processes can be recycled and it can be used back [17], [18]. The small products can be printed using 3D printer with small cost compared to traditional manufacturing process. However, the cost of the large parts in 3D printer is high compared to the traditional manufacturing method [19], [20]. The 3D printing technique is on board from the last three decades, but it is still an under developing technology. This technique requires deep research to get more information so that it extends can be understood and the benefits of this technology can be increased.

There are number of raw materials being used in additive manufacturing processes include metals, alloys, plastics, and other substances in the form of liquids, sheets, powders, and filaments for various applications. Titanium alloys have been electron and laser beam printed and studied for biomedical and mechanical response [21], [22]. The thermoplastic filaments are most commonly used in Fused deposition modelling to fabricate the 3D parts. These materials include acrylonitrile butadiene styrene (ABS), polycarbonate (PC), polylactide (PLA) and Polyamide (PA)[23], [24]. PLA is the one of the most popular materials in 3D printing due to its low cost, good stiffness and strength, high reliability and good dimensional accuracy and surface finish [13] [14]. PLA is a polymer, called polylactic acid which made from the organic and renewable resource such as potato starch and sugar cane. It is easy to print with, compared to other 3D printer material such as ABS. It is strong but more brittle compared to ABS [27]. It has low coefficient of

thermal expansion which limits its applications where the printed part is exposed to temperature higher than 50 °C [16] [17].

Fused deposition modelling (FDM) is one of the popular AM techniques for fabricating plastic parts due to its low cost, minimal wastage and ease of material change [20]. However, FDM is a complex process which is based on many parameters [30], [31]. These parameters can be categorised into four groups such as, part depositing parameters, FDM machine settings, filament properties and environmental factors. Part depositing parameters are infill speed, infill pattern, layer thickness, raster angles, raster width, air gap and contour width. FDM machine settings include nozzle temperature, nozzle diameter, print bed temperature. Filament material properties include its density and colour. Environmental factors include temperature and humidity [32]. Any small change of these process parameters can influence the part quality and material properties. There are limited investigations have been reported on the effect of FDM process parameters on material properties. Therefore, it is crucial to investigate FDM process parameters to ensure the good quality of the parts using this technique. Different studies investigated different 3D printing process parameters and identified their influence on material properties and its behaviour. The raster width and air gaps had been identified as important parameters in affecting the material porosity and mechanical strength [33]. The one of the previous studies pointed out the five important process parameters (layer thickness, orientation, raster angle, raster width and air gap) that have large influence tensile, flexure and impact strength of 3D printed part made up with ABS material [34]. In another study, the two raster orientations, one is cross (0°/90°) and other one is crisscross (45°/-45°) direction were investigated using ABS material and found crisscross (45°/-45°) orientations provides better material strength compared to the other orientation [35]. In another previous study, the effect of layer height, infill density, layer orientation on the mechanical properties of PLA and ABS were investigated and identified that PLA is more suitable for the use of 3D printing material [36]. Letcher et al [37] investigated the three raster orientations 0°, 45° and 90° using PLA material and identified that the 45° raster orientation provided a strongest material behaviour. However, it was not identified that the material behaviour when the raster angle is gradually increased from 0° to 90°. What are microstructural changes occurred within the 3D parted part while using different raster angles.

Raster orientation is one of the most important parameters of FDM 3D printing process. Raster orientation – part build orientation refers to the inclination of a part in a build platform with respect to X, Y and Z axis as shown in Figure 1. The X and Y axes represent the plane parallel to build platform and Z axis represents the vertical plane along the direction of the part build [34]. In this study, part depositing parameter – raster orientation is studied and five different raster orientation angles (0°, 30°, 45°, 60° and 90°)

are investigated, and three specimens with each raster angle orientation setting are printed. The tensile test is performed for each 3D printed specimen and the effects of this process parameter is investigated on its tensile strength. The micro structural analysis on fracture interface of the specimens after tensile testing are also performed using the scanning electron microscope to explain material failure modes and reasons. In this study, the micro-level structural changes on outer and inner surfaces of the 3D parts that are fabricated using the five different raster orientations are also examined in detail.

## II. EXPERIMENTAL PROCEDURES

For this study, the experimental work consists of preparation of standardised tensile test specimens using 3D printer, testing of 3D printed specimens and detailed microstructural analysis of outer and inner surfaces of 3D printed specimens. The information about each step is provided below in detail.

### A. The 3D printing process

First, 3D printed test specimens were created in accordance with the specifications. For that, the test specimen's three-dimensional virtual shape was created using the 3D CAD Solid Works 2019 programme. Figure 2 illustrates the specimen's geometry, which was created in accordance with the ASTM D638 standard tensile test specimen [39]. After creating the geometry for the virtual specimen, the Solid Works file was converted to STL. This format can be used to physically print the specimen on the 3D printer. The STL file was then uploaded to the PC that was controlling the 3D printer. The specimens were printed using the powerful, user-friendly, and dependable Ultimaker 5 3D printer, as seen in Figure 3. It is controlled using a touch screen interface that shows thorough status information. The specimens are printed using the PLA spool, as seen in Figure 4. Cura 4.3.0 - The SolidWorks-created design was prepared for 3D printing using 3D printing software. This software can monitor the status of printers, plan maintenance, queue prints, and manage various software designs. To have comprehensive control over the printing programme and to print with precise printing parameter settings, such as varied raster orientations, custom printing settings were employed. In order to prevent warping on the initial layer of the specimen, this 3D printer extruded the material at 200°C at a speed of 70 mm/s with the heated bed surface at 60°C. As seen in Figure 5, the samples were printed with five different raster orientation angles: 0°, 30°, 45°, 60°, and 90°. Each raster orientation was employed with a 100% infill density. With each raster orientation, three identical tensile specimens were printed, for a total of 18 specimens. These samples were all constructed using a 1 kg spool of PLA material. This printer starts a printing with the build of a thin layer of base support as shown in Figure 6 and then it builds an outer layer base and fill the specimen with specific raster orientation. The process of the 3D printing for these tensile specimens is shown in Figure 1.1.

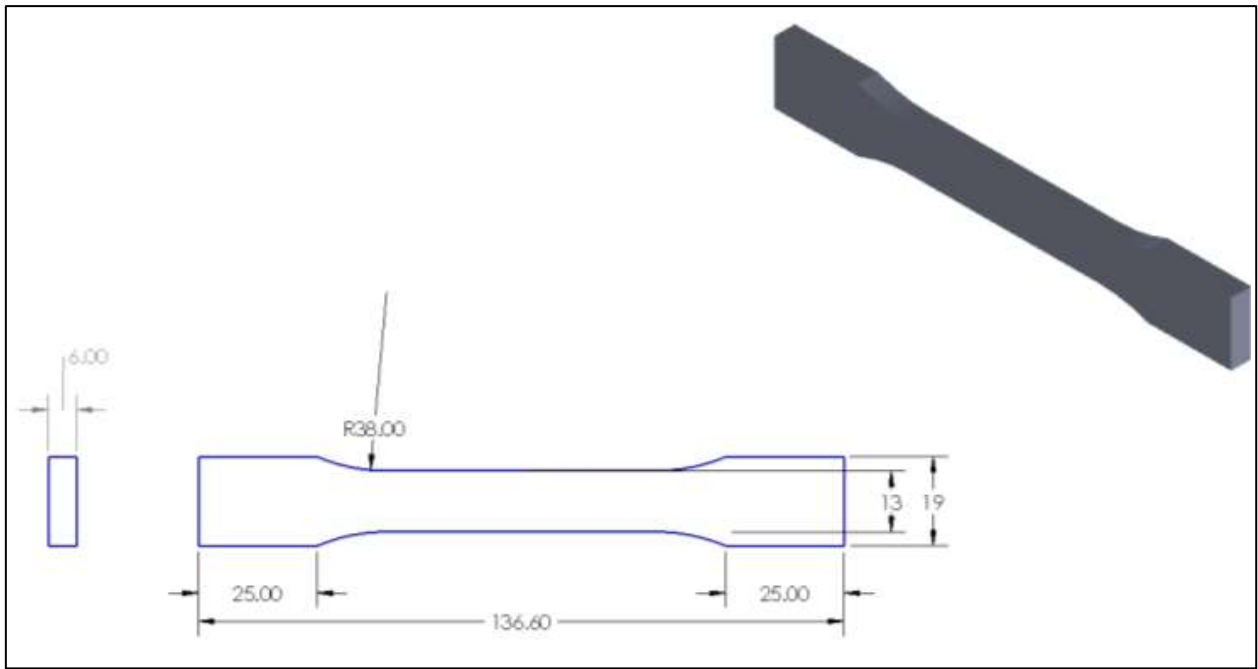


Fig. 1.1: Geometry of the tensile test specimen according to ASTM D638 standard (all dimensions are in mm).

shown in Table 3 and the summary of all the tensile test results are given in Table 4.

### III. RESULTS AND DISCUSSIONS

#### A. Tensile Test

There are three identical tensile specimens were tested with each raster orientation. The individual results for each test are

Raster Orientation (degree)	Actual Width (mm)	Actual Thickness (mm)	Elongation at Break (%)	Modulus Elasticity (GPa)	Ultimate Stress (MPa)
0° (1)	13.36	6.06	1.38	1.23	13.92
0° (2)	13.41	6.02	2.111	0.95	15.36
0° (3)	13.41	6.02	2.25	0.95	13.43
30° (1)	13.39	6.05	3.1	0.87	21.27
30° (2)	13.45	6.07	1.92	1.02	14.69
30° (3)	13.38	6.08	2.24	0.95	16
45° (1)	13.02	5.91	4.47	1.31	54.15
45° (2)	12.96	5.89	3.96	1.59	54.21
45° (3)	12.99	5.93	4.37	1.77	58.61
60° (1)	13.37	6.07	1.85	0.89	13.91
60° (2)	13.31	6.09	2.21	1.05	17.01
60° (3)	13.41	6.06	2.06	0.98	15.51
90° (1)	13.37	6.02	3.66	1.83	47.21
90° (2)	13.41	6.1	3.28	1.91	42.71
90° (3)	13.35	6.02	2.54	1.57	31.71

Table 5.1: Tensile test results of 3D printed specimens.

Raster Orientation (degree)	Elongation at Break (%)	Modulus Elasticity (GPa)	Ultimate Stress (MPa)
0°	2.08	1.04	14.53
30°	2.59	0.95	17.61
45°	4.44	1.56	55.95
60°	2.21	0.97	15.77
90°	3.33	1.77	40.83

Table 5.2: The summary of all the tensile test results

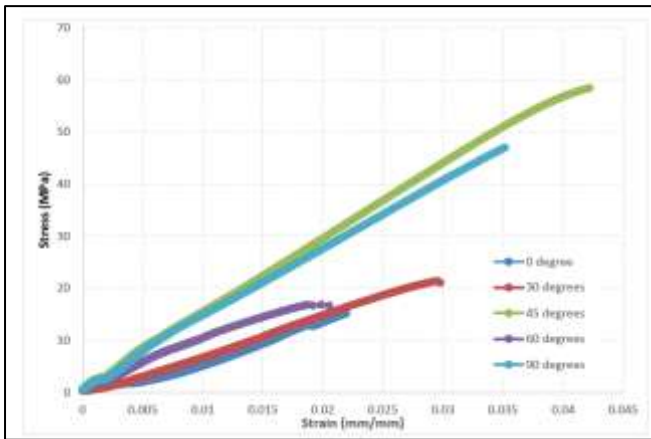


Figure 5.1: Tensile test results (stress-strain curves) for each of the raster orientation.

Table 3 and Table 4 results show the effect of raster orientation on tensile properties including the ultimate strength, the modulus of elasticity and elongation at break that for the material of PLA. The 45° raster orientation produced a strongest specimen with the average ultimate tensile is 55.45 MPa and highest elongation of 4.24 %. The 90° raster orientations produced the specimen with the average ultimate tensile strength is 40.33 MPa (27% less than the strength of the specimen produced with 45° raster orientation), which is the second highest strength compared to the results of all other printed specimens. The 0°, 30° and 60° orientations produced weak specimens with the average ultimate strength are 14.04 MPa, 17.11 MPa and 15.27 MPa respectively. These results show that the position of raster is

an important parameter for 3D printing, and it has a vital role in the specimen strength. Figure 5.1 shows the stress strain curves for the specimens printed with five different raster orientations. From these curves it can be identified that which specimen have strongest, toughest and brittle material behaviour. In order to identify which orientation produced a strongest specimen, the stress value at break are compared for all these five specimens. The orientation 45° shown a strongest specimen with the value of 55.45 MPa and specimen printed with the orientation of 0° produced a weakest specimen with the value of 14.03 MPa. The specimen printed with the orientations of 45°, 90° and 60° shown both elastic and plastic deformation, therefore these specimens are identified as hard materials. The specimen printed with the orientations of 30° and 0° deformed only elastically and show brittle material behaviour. The toughness is the measure of material's ability to absorb energy before it breaks and it can be measured by the area under the stress strain curve. In term of identifying toughest specimens among all these five specimens, Figure 5.1 shows that the specimen printed with the orientations of 45° produced a specimen with high toughness, and for the specimen with the orientations of 90°, 30°, 60° and 0° produced specimens with gradually reduction of the value of toughness from high to low respectively.

#### B. Outer surface observations of tensile specimens

Figure 5.2 shows SEM micrographs of outer top surfaces of the tensile specimens. These micrographs confirmed the printed patterns formed with five different raster orientations.

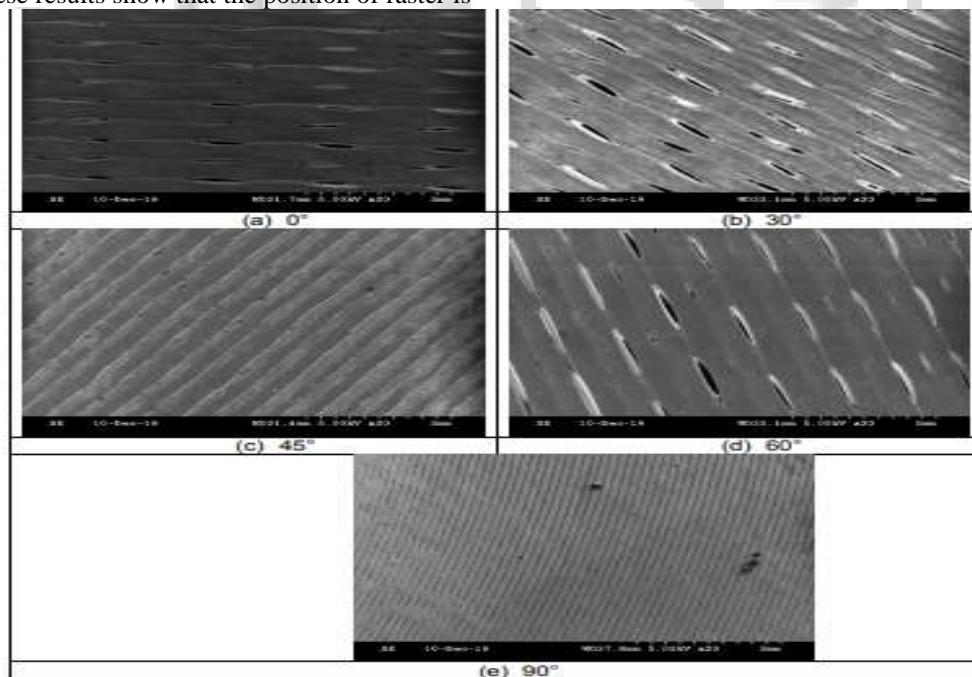


Fig. 5.2: SEM micrographs represent printing patterns those are formed with five different raster orientations (a) 0°, (b) 30°, (c) 45°, (d) 60° and (e) 90°.

After a tensile test, observations at the fracture interface Figure 5.3 displays SEM micrographs of tensile specimen fracture interfaces at five different raster angles: 0°, 30°, 45°, 60°, and 90°. The specimens failed due to poor interfacial adhesion between the layers, as shown in Figure 5.3 (a, b, and d), which shows that the raster angles of 0°, 30°, and 60° did not give the material the chance to resist the tensile load. Instead, the specimens ruptured along the layers and formed smooth fractured surfaces. These raster orientations did not properly transfer tensile load from one layer to another, resulting in the specimens' low tensile strength and tensile modulus. The specimens formed with the

and 60° did not give the material the chance to resist the tensile load. Instead, the specimens ruptured along the layers and formed smooth fractured surfaces. These raster orientations did not properly transfer tensile load from one layer to another, resulting in the specimens' low tensile strength and tensile modulus. The specimens formed with the

45° and 90° raster angles, on the other hand, exhibit rough fractured surfaces as shown in Figure 5.3(c) and (e), and these specimens are highlighted as a result of material failure

during tensile loading, which led to the achievement of greater tensile strength and tensile modules.

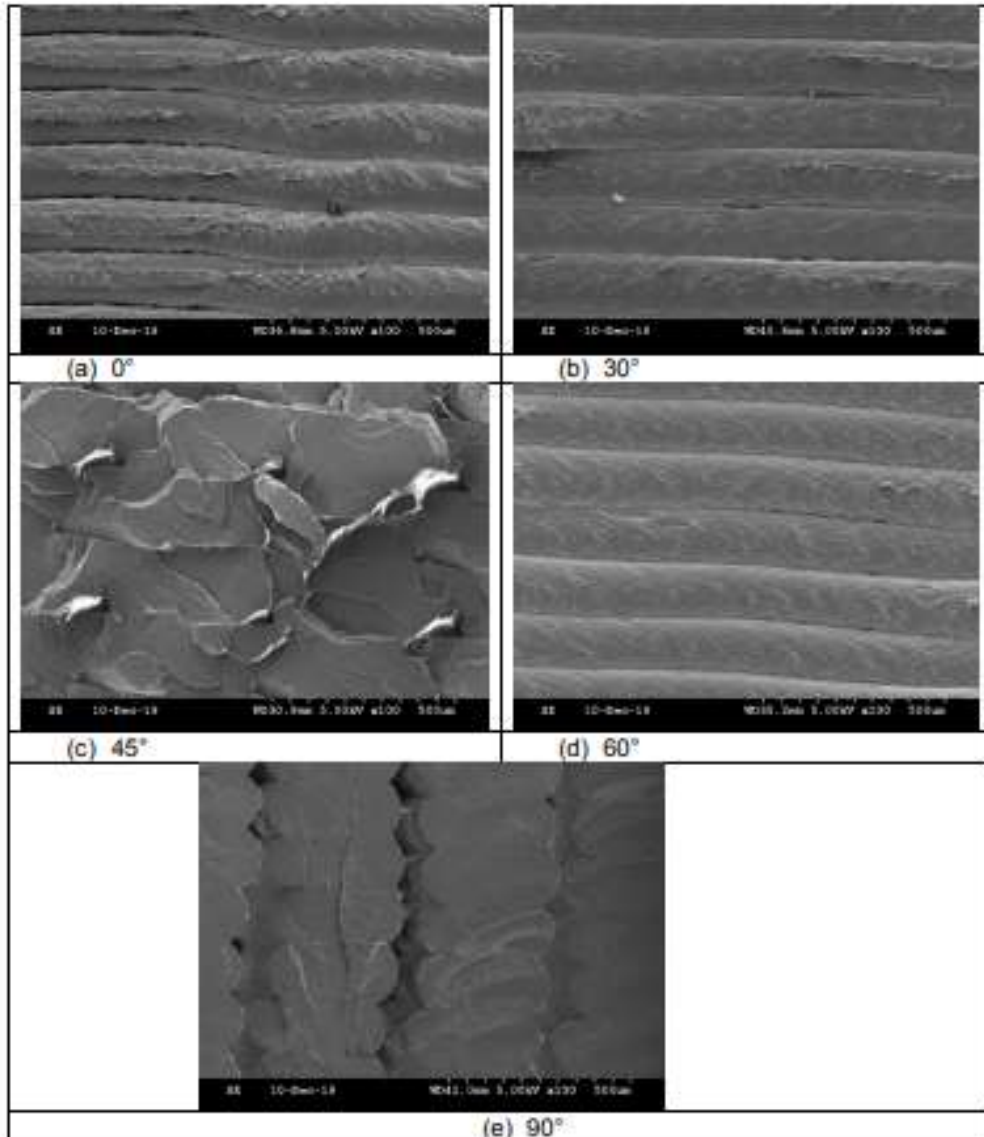


Fig. 5.3: SEM images of fractured interface of tensile specimens with five raster angles a. 0°, b. 30°, c. 45°, d. 60° and e. 90°.

Defects in 3D printing Any flaws in 3D printed parts, such as holes, cracks, voids, and air gaps, have a negative impact on the material qualities of the part. Therefore, it is necessary to prevent these flaws in the 3D printed part's ultimate finished shape. In this study, these flaws in 3D printed specimens that were created using five distinct raster orientations are found utilizing SEM microstructure pictures. The exterior top surfaces of all five specimens are shown in Figure 5.4's SEM microstructure photographs, which reveals various issues with the print quality. The examples printed with the 0°, 30°, and 60° raster angles as illustrated in Figure 5.4 (a), (b), and (c) exhibit the most noticeable issues (d). These specimens' exterior surfaces revealed cracks between two rasters. These rasters weren't correctly bonded to one another during printing, which resulted in inner layer cracks on the printed specimens'

outside faces. The specimens produced with 0°, 30°, and 60° raster orientations have average crack lengths of 0.7 mm, 0.8 mm, and 1.2 mm, respectively. It demonstrated that as compared to specimens printed at raster angles of 0° and 30°, specimens printed at 60° exhibited more cracks. Rapid heating and cooling create non-uniform temperature gradients and thermal tensions within the material throughout the 3D printing process. These pressures result in fissures between two neighbouring rasters or deformations in the inner layer, which lead to dimensional error and delamination. In comparison to the other two raster angles, the specimen with a 60° raster angle is more likely to deform due to these forces and produce significant cracks and openings. This may be due to the fact that after melting at a 60° angle, it is more challenging for the material to totally restore its former shape or dimension. As illustrated in

Figures 5.4 (c) and (d), the specimens with raster angles of  $45^\circ$  and  $90^\circ$ , in contrast, generated compact outside surfaces and any flaw cannot be observed on them (e). Also, the curve edge of the tensile specimen fabricated with  $45^\circ$  raster angle is examined by SEM and images are shown in Figure 12. It demonstrates that a raster angle of  $45^\circ$  produced 3D prints of high quality and resolved issues with the radius section of the tensile specimen that had been noted earlier in the specimen produced with a raster angle of  $0^\circ$  [37]. In order to analyse the internal quality of 3D printed specimens, the fracture interface of each of the five tensile specimens that were created with five distinct raster orientations was examined. The SEM images for each of the five fracture surfaces that developed following the tensile test are shown in Figure 5.5. These photographs revealed a number of issues with the 3D printing process' layer positioning. Figure 5.5 (a), (b), and (c) show that the specimens made with raster orientations of  $0^\circ$ ,  $30^\circ$ , and  $60^\circ$  created a series of air gaps between the layers along the thickness of the specimen (d). The specimen formed with a raster angle of  $60^\circ$  is shown in Figure 5.5(e), and it clearly identifies the air gaps in the positioning of the layers and to adjacent rasters. Additionally, the fracture interface of the specimen printed with a  $45^\circ$  raster angle is shown in Figure 5.5 (c), which also reveals the triangular voids, which are on average 2200 m2 in size, between the two layers. The fracture interface of the specimen printed with a  $90^\circ$  raster angle is similarly depicted in Figure 5.5 (f), which also shows the diamond-shaped openings, which average 18000 m2 in

size, between the two layers. Temperature changes throughout the layering process might result in these flaws in 3D printed specimens. In the FDM technique, the 3D printer deposits the filaments layer by layer, and these layers are joined together by localised re-melting of previously hardened material. These apertures, air gaps, and voids may develop as a result of the printing process' uneven heating and cooling. This uneven temperature gradient creates irregular strains and deformations [34]. Overall, the specimens produced with raster orientations of  $0^\circ$ ,  $30^\circ$ , and  $60^\circ$  revealed printed flaws on the specimens' outer and interior surfaces. These flaws had a direct impact on the material strength of the specimen and resulted in weaker specimens. When compared to specimens made with raster orientations of  $90^\circ$  and  $45^\circ$ , the specimens made with raster orientations of  $0^\circ$ ,  $30^\circ$ , and  $60^\circ$  showed inferior tensile strength. Nevertheless, the specimens made with raster orientations of  $90^\circ$  and  $45^\circ$  had good outside surfaces, and any flaws couldn't be observed on their outer sides. On the fracture edges of these specimens, however, certain internal flaws can still be observed. It is obvious that by avoiding these printing issues and flaws, the strength of these specimens can be increased even more. Raster orientation thus influences the strength, accuracy, and surface quality of 3D printed parts. By decreasing the gaps between the deposited layers and improving surface smoothness, a part's strength can be increased with the proper selection of this angle, especially for challenging parts like curved surfaces.

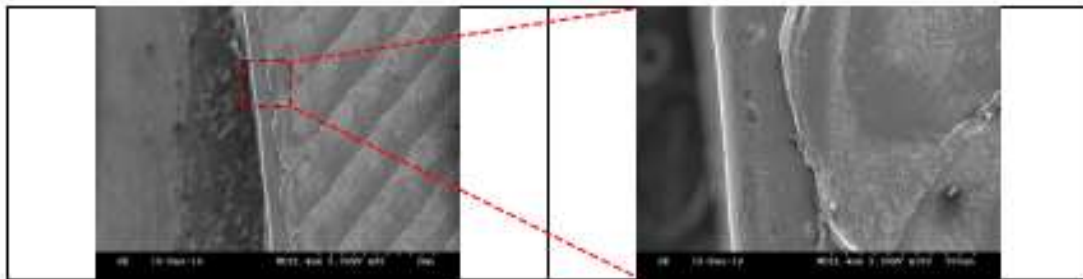


Fig. 5.4: SEM images of the curve edge of the tensile specimen fabricated with  $45^\circ$  raster angle.

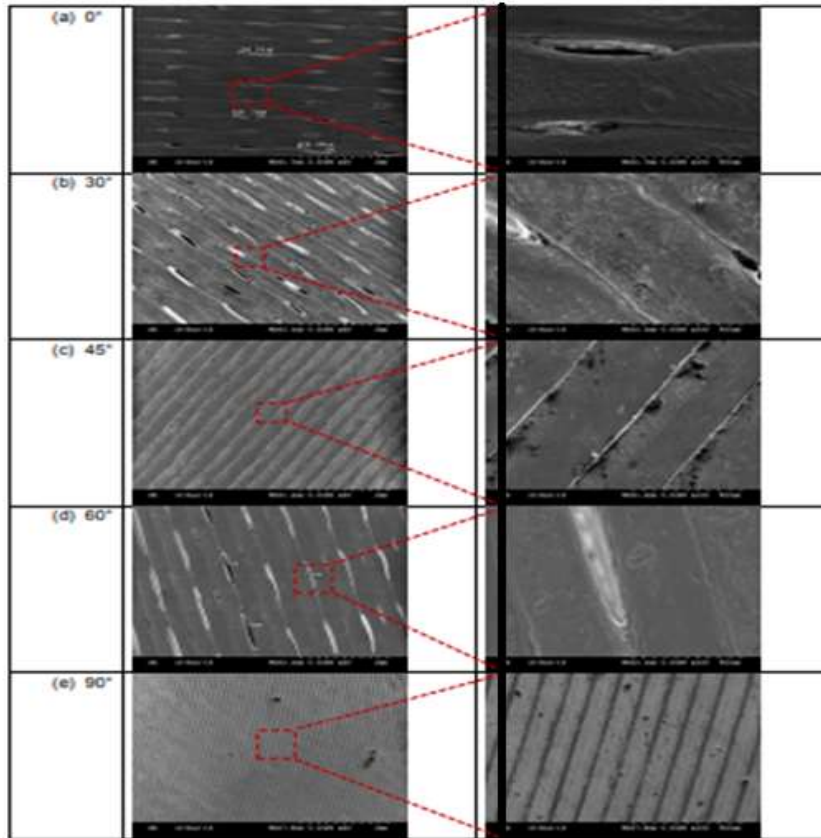


Fig. 5.4: SEM images of outer surface of the specimens show the defects-openings or cracks for the orientation of 0°, 30°, 45°, 60° and 90°.

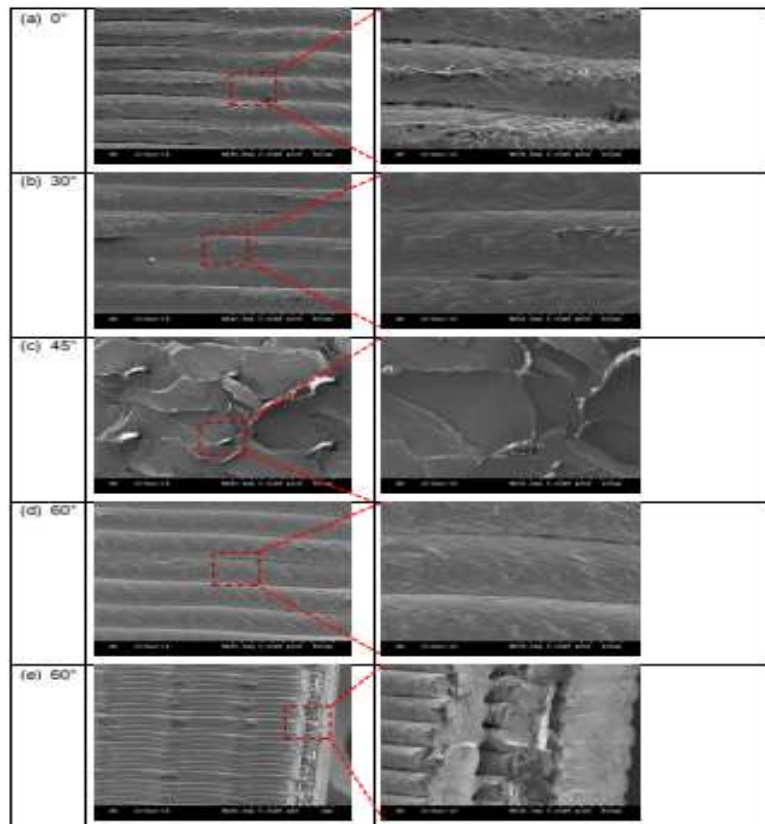


Fig. 5.5: SEM images show the fracture interface formed after tensile test of the specimens fabricated with five different raster orientations.

#### IV. CONCLUSION

In this work, PLA material was employed to construct the 3D printed specimens at each of the five distinct raster angles. To find the ideal raster position to create the sturdiest 3D printed object, the tensile characteristics of each of these examples were examined. In order to clarify the modes and causes of material failure, the fracture interface of these specimens after tensile testing was further investigated using a scanning electron microscope (SEM). This study also evaluated the micro-level structural alterations brought about by the employment of various raster orientations on the outside and inner surfaces of these 3D printed specimens. From this investigation, the following findings can be derived.

The strength, precision, and surface smoothness of the printed specimens are significantly influenced by the raster location, which is a key process parameter for 3D printing. The strongest specimen was generated by the 45° raster orientation, with a maximum elongation of 4.24 percent and an average ultimate tensile of 55.45 MPa. Among all printed specimen results, the 90° raster orientation produced the second-highest strength.

The specimens manufactured with the raster angles of 0°, 30°, and 60° formed smooth fractured surfaces, indicating that the specimens with these orientations do not provide the material with the opportunity to resist the tensile load; rather, the specimens failed due to inadequate interfacial adhesion between the layers, resulting in lower values of tensile strength and tensile module. The specimens made with the 45° and 90° raster angles, however, had rough cracked surfaces and were broken as a result of the material failing under tensile loading, which resulted in higher tensile strength and tensile modules.

The results of the microstructural examination showed that the specimens printed with the 0°, 30°, and 60° raster angles had cracks between the two rasters on their exterior surfaces. The examples with raster angles of 45° and 90°, in contrast, formed compact outside surfaces that offer a better surface quality. A sequence of air gaps and voids between the layers were seen along the specimens' thickness in the micro level inspections of the fracture interface (inner surfaces) of all five specimens.

The specimens produced with raster orientations of 0°, 30°, and 60° revealed a number of printing flaws on the specimens' outer and interior surfaces. While the specimens made with raster orientations of 90° and 45° generated compact outer surfaces, any flaws on them cannot be observed at the microscopic level, and therefore offer greater surface smoothness. On the fracture edges of these specimens, however, certain internal flaws can still be observed. The findings of the tensile strength tests can be connected with these microstructural observations. By avoiding printing issues and flaws, 3D parts' strength and precision can be increased still further.

#### REFERENCES

[1] Y. L. Yap, C. Wang, S. L. Sing, V. Dikshit, W. Y. Yeong, and J. Wei, 'Material jetting additive manufacturing: An experimental study using designed metrological

benchmarks', *Precision engineering*, vol. 50, pp. 275–285, 2017.

[2] N. Gupta, C. Weber, and S. Newsome, 'Additive manufacturing: status and opportunities', *Science and Technology Policy Institute, Washington*, 2012.

[3] T. D. Ngo, A. Kashani, G. Imbalzano, K. T. Nguyen, and D. Hui, 'Additive manufacturing (3D printing): A review of materials, methods, applications and challenges', *Composites Part B: Engineering*, vol. 143, pp. 172–196, 2018.

[4] K. C. Nune, A. Kumar, R. D. K. Misra, S. J. Li, Y. L. Hao, and R. Yang, 'Functional response of osteoblasts in functionally gradient titanium alloy mesh arrays processed by 3D additive manufacturing', *Colloids and Surfaces B: Biointerfaces*, vol. 150, pp. 78–88, 2017.

[5] K. C. Nune, R. D. K. Misra, S. J. Li, Y. L. Hao, and R. Yang, 'Osteoblast cellular activity on low elastic modulus Ti–24Nb–4Zr–8Sn alloy', *Dental Materials*, vol. 33, no. 2, pp. 152–165, 2017.

[6] B. Utela, D. Storti, R. Anderson, and M. Ganter, 'A review of process development steps for new material systems in three dimensional printing (3DP)', *Journal of Manufacturing Processes*, vol. 10, no. 2, pp. 96–104, 2008.

[7] J. Kietzmann, L. Pitt, and P. Berthon, 'Disruptions, decisions, and destinations: Enter the age of 3-D printing and additive manufacturing', *Business Horizons*, vol. 58, no. 2, pp. 209–215, 2015.

[8] H. Lipson and M. Kurman, *Fabricated: The new world of 3D printing*. John Wiley & Sons, 2013.

[9] K. C. Nune, R. D. K. Misra, S. M. Gaytan, and L. E. Murr, 'Biological response of next-generation of 3D Ti-6Al-4V biomedical devices using additive manufacturing of cellular and functional mesh structures', *J Biomater Tissue Eng*, vol. 4, no. 10, pp. 755–771, 2014.

[10] K. C. Nune, R. D. K. Misra, S. J. Li, Y. L. Hao, and R. Yang, 'Cellular response of osteoblasts to low modulus Ti-24Nb-4Zr-8Sn alloy mesh structure', *Journal of Biomedical Materials Research Part A*, vol. 105, no. 3, pp. 859–870, 2017.

[11] T. Boland, T. Xu, B. Damon, and X. Cui, 'Application of inkjet printing to tissue engineering', *Biotechnology Journal: Healthcare Nutrition Technology*, vol. 1, no. 9, pp. 910–917, 2006.

[12] X. Li *et al.*, '3D-printed biopolymers for tissue engineering application', *International Journal of Polymer Science*, vol. 2014, 2014.

[13] S. Yang, K.-F. Leong, Z. Du, and C.-K. Chua, 'The design of scaffolds for use in tissue engineering. Part II. Rapid prototyping techniques', *Tissue engineering*, vol. 8, no. 1, pp. 1–11, 2002.

[14] A. Kumar, K. C. Nune, L. E. Murr, and R. D. K. Misra, 'Biocompatibility and mechanical behaviour of three-dimensional scaffolds for biomedical devices: process–structure–property paradigm', *International Materials Reviews*, vol. 61, no. 1, pp. 20–45, 2016.

[15] A. Kumar, K. C. Nune, and R. D. K. Misra, 'Biological functionality and mechanistic contribution of extracellular matrix-ornamented three dimensional Ti-6Al-4V mesh scaffolds', *Journal of Biomedical*

- Materials Research Part A*, vol. 104, no. 11, pp. 2751–2763, 2016.
- [16] A. Kumar, K. C. Nune, and R. D. K. Misra, 'Biological functionality of extracellular matrix-ornamented three-dimensional printed hydroxyapatite scaffolds', *Journal of Biomedical Materials Research Part A*, vol. 104, no. 6, pp. 1343–1351, 2016.
- [17] Q. Shi *et al.*, 'Recyclable 3D printing of vitrimer epoxy', *Materials Horizons*, vol. 4, no. 4, pp. 598–607, 2017.
- [18] X. Tian, T. Liu, Q. Wang, A. Dilmurat, D. Li, and G. Ziegmann, 'Recycling and remanufacturing of 3D printed continuous carbon fiber reinforced PLA composites', *Journal of cleaner production*, vol. 142, pp. 1609–1618, 2017.
- [19] B. P. Conner *et al.*, 'Making sense of 3-D printing: Creating a map of additive manufacturing products and services', *Additive Manufacturing*, vol. 1, pp. 64–76, 2014.
- [20] C. C. Kai, L. K. Fai, and L. Chu-Sing, *Rapid prototyping: principles and applications in manufacturing*. World Scientific Publishing Co., Inc., 2003.
- [21] S. Zhao *et al.*, 'Compressive and fatigue behavior of functionally graded Ti-6Al-4V meshes fabricated by electron beam melting', *Acta Materialia*, vol. 150, pp. 1–15, 2018.
- [22] L.-C. Zhang, H. Attar, M. Calin, and J. Eckert, 'Review on manufacture by selective laser melting and properties of titanium based materials for biomedical applications', *Materials Technology*, vol. 31, no. 2, pp. 66–76, 2016.
- [23] L. Novakova-Marcincinova, J. Novak-Marcincin, J. Barna, and J. Torok, 'Special materials used in FDM rapid prototyping technology application', in 2012 IEEE 16th International Conference on Intelligent Engineering Systems (INES), 2012, pp. 73–76.
- [24] P. Dudek, 'FDM 3D printing technology in manufacturing composite elements', *Archives of Metallurgy and Materials*, vol. 58, no. 4, pp. 1415–1418, 2013.
- [25] A. Lanzotti, M. Grasso, G. Staiano, and M. Martorelli, 'The impact of process parameters on mechanical properties of parts fabricated in PLA with an open-source 3-D printer', *Rapid Prototyping Journal*, vol. 21, no. 5, pp. 604–617, 2015.
- [26] B. Wittbrodt and J. M. Pearce, 'The effects of PLA color on material properties of 3-D printed components', *Additive Manufacturing*, vol. 8, pp. 110–116, Oct. 2015, doi: 10.1016/j.addma.2015.09.006.
- [27] M. N. Hafsa, M. Ibrahim, M. Wahab, and M. S. Zahid, 'Evaluation of FDM pattern with ABS and PLA material', in *Applied Mechanics and Materials*, 2014, vol. 465, pp. 55–59.
- [28] J. Jiang, L. Su, K. Zhang, and G. Wu, 'Rubber-toughened PLA blends with low thermal expansion', *Journal of Applied Polymer Science*, vol. 128, no. 6, pp. 3993–4000, 2013.
- [29] J. Hughes, R. Thomas, Y. Byun, and S. Whiteside, 'Improved flexibility of thermally stable poly-lactic acid (PLA)', *Carbohydrate polymers*, vol. 88, no. 1, pp. 165–172, 2012.
- [30] J. Comb, W. Priedeman, and P. W. Turley, 'FDM® Technology process improvements', in 1994 International Solid Freeform Fabrication Symposium, 1994.
- [31] R. H. Sanatgar, C. Campagne, and V. Nierstrasz, 'Investigation of the adhesion properties of direct 3D printing of polymers and nanocomposites on textiles: Effect of FDM printing process parameters', *Applied Surface Science*, vol. 403, pp. 551–563, 2017.
- [32] O. A. Mohamed, S. H. Masood, and J. L. Bhowmik, 'Optimization of fused deposition modeling process parameters: a review of current research and future prospects', *Advances in Manufacturing*, vol. 3, no. 1, pp. 42–53, 2015.
- [33] K. Chin Ang, K. Fai Leong, C. Kai Chua, and M. Chandrasekaran, 'Investigation of the mechanical properties and porosity relationships in fused deposition modelling-fabricated porous structures', *Rapid Prototyping Journal*, vol. 12, no. 2, pp. 100–105, 2006.
- [34] A. K. Sood, R. K. Ohdar, and S. S. Mahapatra, 'Parametric appraisal of mechanical property of fused deposition modelling processed parts', *Materials & Design*, vol. 31, no. 1, pp. 287–295, 2010.
- [35] A. W. Fatimatuzahraa, B. Farahaina, and W. A. Y. Yusoff, 'The effect of employing different raster orientations on the mechanical properties and microstructure of Fused Deposition Modeling parts', in 2011 IEEE Symposium on Business, Engineering and Industrial Applications (ISBEIA), 2011, pp. 22–27.
- [36] A. Rodríguez-Panes, J. Claver, and A. M. Camacho, 'The Influence of Manufacturing Parameters on the Mechanical Behaviour of PLA and ABS Pieces Manufactured by FDM: A Comparative Analysis', *Materials*, vol. 11, no. 8, p. 1333, Aug. 2018, doi: 10.3390/ma11081333.
- [37] T. Letcher and M. Waytashek, 'Material property testing of 3D-printed specimen in PLA on an entry-level 3D printer', in ASME 2014 international mechanical engineering congress and exposition, 2014, p. V02AT02A014–V02AT02A014.
- [38] 'GoPrint3D - 3D Printer Specialists'. [Online]. Available: <https://www.goprint3d.co.uk>. [Accessed: 17-Dec-2019].
- [39] D20 Committee, 'Test Method for Tensile Properties of Plastics', ASTM International.